Effect of Pressure on the Proton-Transfer Rate from a Photoacid to a Solvent. 2. DCN2 in Propanol

Liat Genosar, Pavel Leiderman, Nahum Koifman, and Dan Huppert*

Raymond and Beverly Sackler Faculty of Exact Sciences, School of Chemistry, Tel Aviv University, Tel Aviv 69978, Israel

Received: April 24, 2003; In Final Form: October 2, 2003

The reversible proton dissociation and geminate recombination of photoacids is studied as a function of pressure in liquid propanol. For this purpose we used a strong photoacid, 5,8-dicyano-2-naphthol (DCN2) ($pK_a^* \sim -4.5$ in water), capable of transferring a proton to alcohols. The time-resolved emission data are explained by the reversible diffusion-influenced chemical reaction model. At low pressure, the proton-transfer rate slightly increases with pressure whereas, at high pressure, the rate constant decreases significantly as the pressure increases. The pressure dependence is explained using an approximate stepwise two-coordinate proton-transfer model. The model is compared with the Landau−Zener curve-crossing proton tunneling formulation. Decrease of the proton-transfer rate at high-pressures reflects the solvent-controlled limit, and the increase in rate at low-pressures reflects the proton tunneling nonadiabatic limit. The results are compared with our recent studies of the pressure dependence of proton transfer from 2-naphthol-6-sulfonate (2N6S) to water and DCN2 to ethanol. Though in 2N6S−water, the proton transfer is controlled by proton tunneling, in our current work we find that, at high pressure, the solvent controls the rate of the process.

Introduction

Excited-state proton transfer (ESPT) from a photoacid molecule[1−5] was used in studies of proton-transfer reactions in liquids and solids. Recent studies on the proton-transfer rate to the solvent[6−13] emphasize the dual role played by the solvent molecule (1) as a proton acceptor and (2) as a solvating medium of both the reactant and the product.[14−16]

Theoretical studies revealed that tunneling is the dominant reaction mode for proton transfer, even at ambient temperatures. The theory of the proton-transfer reaction in solution was developed by Dogonadze, Kuznetzov, Ulstrup, and co-workers[17,18] and then extended by Borgis and Hynes, Cukier, Voth, and Hammes-Schiffer.[19−22] These theories show that the presence of a potential energy barrier in the proton-reaction coordinate causes tunneling through the barrier in the reaction pathway, as opposed to passage over the barrier.

Ando and Hynes[15] studied the acid ionization of HCl in water via a combination of electronic structure calculations and Monte Carlo computer simulations. The mechanism is found to involve: first, an activationless (or nearly so) motion in a solvent coordinate, which is adiabatically followed by the quantum proton, produces a "contact" ion pair Cl^- H_3O^+, which is stabilized by ∼7 kcal/mol; second, motion in the solvent with a small activation barrier, as a second adiabatic proton transfer produces a "solvent-separated" ion pair from the "contact" ion pair in a nearly thermoneutral process.[15]

The Landau−Zener model is well studied for microscopic treatment of proton transfer. Hammes-Schiffer[22,23] and co-workers developed a method to calculate the rate of proton transfer based on molecular dynamics with quantum transitions (MDQT), which are mixed quantum/classical surface hopping methods that incorporate nonadiabatic transitions between the proton vibration and/or electronic states. The advantages of MDQT are that it accurately describes branching processes (i.e., processes involving multiple pathways), is valid in the adiabatic and nonadiabatic limits and the intermediate regime, and provides real-time dynamics information.

The theory for nonadiabatic proton transfer is very similar to the theory for nonadiabatic electron transfer in its treatment of the involvement of the solvent. In the model,[17] when the polar solvent is equilibrated to the reactant (the bottom of the potential well) the proton will not be transferred due to an energy mismatch in the reactant and product states. Upon solvent fluctuation, the energy of the reactant and product states becomes equal and it is in this solvent configuration that the proton tunnels from one side of the well to the other. Finally, upon solvent relaxation, the product state is formed.

If the pretunneling and posttunneling configurations are regarded as real transient chemical intermediates, the process can be described by a set of three consecutive chemical equations[24] denoted as (a), (b), and (c) in Scheme 1. We also plot the potential surface diagram for the particular chemical equation.

AH is the protonated photoacid, S_B a single solvent molecule to which the proton is transferred, S_R the solvent configuration to stabilize the reactants, and S_p the solvent configuration of the products. $S^{\neq}$ is the solvent configuration to equally stabilize $AH\cdots S_B$ and $A^- \cdots HS_B^+$. The first equation describes the motion of the solvent configuration to reach the activation solvent configuration. The second equation describes the tunneling process in the proton coordinate, Q_H. This process occurs when the energies of the reactant and product states become equal. The third equation describes the solvent configuration relaxation toward the bottom of the product well.

* Corresponding author. E-mail: huppert@tulip.tau.ac.il. Fax/phone: 972-3-6407012.

10.1021/jp035099l CCC: $27.50
Published on Web 12/17/2003

SCHEME 1

(a) $AH+S_B+S_R \underset{k_{-1}}{\overset{k_1}{\rightleftharpoons}} AH\cdot S_B+S^{\neq}$

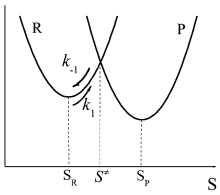

(b) $AH\cdot S_B+S^{\neq} \underset{k_{-2}}{\overset{k_2}{\rightleftharpoons}} A^-\cdot HS_B^+ + S^{\neq}$

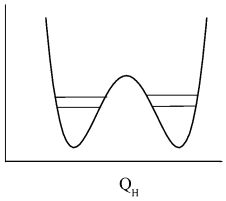

(c) $A^-\cdot HS_B^+ + S^{\neq} \xrightarrow{k_3} A^- + HS_B^+ + S_p$

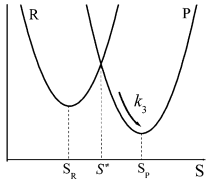

In previous papers,[8−13] we described our experimental results of the unusual temperature dependence of the excited-state proton transfer from several photoacids to liquid water, monols, diols, and glycerol. For DCN2 in methanol and ethanol at temperatures above 285 K, the rate of the proton transfer is almost temperature independent whereas, at $T < 250$ K, the rate exhibits great temperature dependence. The rate constant is similar to the inverse of the longest component of the dielectric relaxation time of a particular protic solvent. We proposed a simple stepwise model to describe and calculate the temperature dependence of the proton transfer to the solvent reaction. The model accounts for the large difference in the temperature dependence, the proton-transfer rate at high and low temperatures and the solvent dependencies. We further studied the temperature dependence of the proton-transfer rate in water using 2-naphthol and 2-naphthol-6,8-disulfonate. The temperature dependence was explained using the same stepwise model.

The unusual temperature dependence studies can also be explained using proton-transfer theory, based on the Landau−Zener curve crossing formulation. The high-temperature behavior of the rate constant denotes the nonadiabatic limit, whereas the low-temperature behavior denotes the adiabatic limit. We used an approximate expression for the proton-transfer rate, which bridges the nonadiabatic and the solvent-controlled adiabatic limit to fit the temperature dependence curve of the experimental proton-transfer rate constant.

Pressure is known to influence the rate of chemical reactions in the condensed phase.[25−30] External pressure changes such properties of the medium and reactants as the reaction free volume, potential energy profile along the reaction path, compressibility, viscosity, and the reorganization energy of the medium. The absolute value of the reaction rate constant and its temperature dependence may depend on all these parameters. The pressure influences both the characteristics of classical over-barrier reactions and the tunneling transfer of the proton. The pressure influence on tunneling in the solid state is discussed in refs 31 and 32. In solids, the tunneling reaction depends exponentially on both the equilibrium distance between the reactants and the frequency of intermolecular vibrations, which varies with compression.

One important difference between electron transfer and proton transfer is the extreme sensitivity of the proton tunneling matrix element to distance. The functional form of the tunneling coupling matrix element between the reactant and product state, for moderate to weak coupling, is

$$C(Q_H) = C_0 \exp(-\alpha\delta Q_H) \qquad (1)$$

The decay parameter, α,[18,19] is very large, 25−35 $Å^{-1}$, in comparison with the corresponding decay parameter for the electronic coupling in electron transfer, 1 $Å^{-1}$. It is this feature that makes the dynamics of proton transfer so sensitive to the internuclear separation of the two heavy atoms, and hence, pressure can be used to gradually change the intermolecular distance. For many liquids, pressure is known to change the liquid and solid density. The volume decreases by approximately 25% at about 10 kbar. Therefore the intermolecular distance changes with pressure.

As a first-order approximation, the change in intermolecular distance, δQ_H, is related to the change in volume, ΔV, as $\sqrt[3]{\Delta V}$. In the strong coupling limit, the tunneling matrix element, C, varies much less rapidly with changing Q_H and is approximately linear. Proton tunneling occurs only when the energies of the reactant and product states become equal. Thus, solvent fluctuation brings the reactant to the crossing point step (a) in Scheme 1.

Time-resolved fluorescence studies of the photoacid 8-hydroxy-1,3,6-pyrenetrisulfonate (HPTS) in water as a function of pressure have been carried out at pressures up to the ice transition point of H_2O.[33] The proton-transfer rates derived from these studies exhibit an increase with pressure from 8×10^9 s^{-1} at 1 atm and 294 K to 2.5×10^{10} s^{-1} at the liquid−ice VI transition point at 9 kbar and 294 K.

In a more recent study,[34] we measured, using time-resolved emission techniques, proton dissociation from a strong photoacid, DCN2, and the reversible geminate recombination processes as a function of pressure in ethanol. The experimental time-resolved fluorescence data were analyzed by the numerical solution of the transient Debye−Smoluchowski equation (DSE). We found that the proton dissociation rate constant, k_{PT}, of excited DCN2 in neat ethanol at relatively low pressures (up to 10 kbar) increases slightly with pressure, whereas at higher pressure up to the freezing point of ethanol, about 1.9 GPa, the proton-transfer rate decreases with pressure and its value in the high pressure regime is similar to the inverse of the dielectric relaxation time. The stepwise two-coordinate model was used successfully to fit the unusual pressure dependence of the proton-transfer rate.

Recently,[35] we also studied the proton-transfer rate from the photoacid 2-naphthol-6-sulfonate to water as a function of pressure. We found that the proton dissociation rate constant, k_{PT}, of excited 2-naphthol-6-sulfonate in water up to the pressure of the freezing point (∼10 kbar), increases with pressure by a factor of about 8. This large rate increase with pressure is about 3 times larger than that found for HPTS.[33] We compared these results with our previous pressure work on DCN2 in ethanol. We used the stepwise two-coordinate model to qualitatively fit the pressure dependence of the proton-transfer rate. Analysis of the experimental data by the model shows that the pressure affects both steps but in opposite directions. The main pressure effect is the decrease of the distance between the proton donor and acceptor. The increase in rate, as a function of pressure, denotes the nonadiabatic limit and also manifests the strong dependence of proton tunneling on the distance between the two heavy atoms which decreases with an increase of pressure.

In this paper we further explore the effect of pressure on excited-state intermolecular proton-transfer (ESPT) dynamics. For this purpose we chose a strong photoacid, DCN2 ($pK^* \sim -4$ in water), and the solvent was a slow relaxing protic liquid, propanol. The main finding of this study is that the proton-transfer rate at low pressures increases slightly. At higher pressures, the proton transfer decreases appreciably as a function of pressure. We used our qualitative stepwise two-coordinate model to explain the strong pressure effect on proton transfer. The model can be related to theories of proton transfer[17,19] based on the Landau−Zener curve crossing formulation.

Experimental Section

Pressurized time-resolved emission was measured in a compact gasketed diamond anvil cell[36] (DAC) purchased from D'Anvil[37,38] with 0.3 carat low-fluorescent high-UV transmission diamonds.

To provide a larger volume of the sample for sufficient fluorescent intensity, a 0.45 mm hole was drilled in the 0.8 mm thick stainless gasket. The low-fluorescence-type diamonds served as anvils. The anvil seats were with suitable circular apertures for the entry and exit of the exciting laser beam and the excited fluorescent intensity. With this cell, pressures up to 30 kbar were reached without detriment to the diamond anvils. The pressure generated was calibrated using the well-known ruby fluorescent technique.[39]

Time-resolved fluorescence was measured using the time-correlated single-photon counting (TCSPC) technique. As an excitation source, we used a continuous wave (cw) mode-locked Nd:YAG-pumped dye laser (Coherent Nd:YAG Antares and a 702 dye laser), providing a high repetition rate (>1 MHz) of short pulses (2 ps at full width half-maximum, fwhm). The (TCSPC) detection system is based on a Hamamatsu 3809U photomultiplier, Tennelec 864 TAC, Tennelec 454 discriminator, and a personal computer-based multichannel analyzer (nucleus PCA-II). The overall instrumental response was about 50 ps (fwhm). Measurements were taken at 10 nm spectral width. Steady-state fluorescence spectra were taken using a SLM AMINCO-Bowman-2 spectrofluorometer.

DCN2 was synthesized by Tolbert and co-workers.[40] The sample concentrations were between 4×10^{-4} and 1×10^{-4} M. Solvents were of reagent grade and were used without further purification. The solution's pH was approximately 6.

The DCN2 fluorescence spectrum consists of two structureless broad bands (~40 nm fwhm). The emission band maximum of the acidic form (ROH*) in water and alcohols emits at 450 nm. The emission band maximum of the alkaline form (RO^-*) in water and alcohols emits at 600 nm. At 450 nm, the overlap of the two-luminescence bands is rather small and the contribution of the RO^-* band to the total intensity at 450 nm is about 1%. In addition, we find some fluorescent impurity in the DCN2 compound that emits in the UV and blue part of the emission spectrum. At 1 atm the impurity emission level is about 1% of the peak intensity at 450 nm and increases to 4% at 20 kbar. The pressure dependence of the background luminescence can arise from dimerization of DCN2 to a nonproton emitting dimer. Therefore, in the time-resolved analysis, we add to the calculated signal an additional component with an exponential decay of about 10 ns, with an amplitude of about 2% at 1 atm, which increases with pressure up to 4% at 20 kbar to account for the impurity fluorescence. To avoid ambiguity, due to the overlap between the fluorescence contributions of ROH* and RO^-*, and to minimize the impurity fluorescence, we mainly monitored the ROH* fluorescence at 480 nm.

Results

Reversible Diffusion-Influenced Two Step Model. Previous studies of reversible ESPT processes in solution led to the development of a reversible diffusion influenced two step model[41,42] (Scheme 2).

Scheme 2

$$\mathrm{ROH}^* \underset{k_r}{\overset{k_{PT}}{\rightleftharpoons}} [\mathrm{RO}^-{}^*\cdots\mathrm{H}^+]_{r=a} \overset{\mathrm{DSE}}{\rightleftharpoons} \mathrm{RO}^-{}^* + \mathrm{H}^+$$

In the continuous diffusion approach, the photoacid dissociation reaction is described by the spherically symmetric diffusion equation (DSE)[43] in three dimensions.[41,42] The boundary conditions at $r = a$ are those of the back-reaction (Scheme 1). k_{PT} and k_r are the "intrinsic" dissociation and recombination rate constants at the contact sphere radius, a. Quantitative agreement was obtained between the model and the experiment.[41,42] A detailed description of the model, as well as the fitting procedure, is given in references 8, 41, and 42.

For the numerical fit, we used the user-friendly graphic program, SSDP (Ver. 2.63), of Krissinel and Agmon.[44] The comparison of the calculated signal with the experimental results involves several parameters. Usually, the adjustable parameters are the proton-transfer rate to the solvent, k_{PT}, and the geminate recombination rate, k_r. The contact radius, a, has acceptable literature values.[43] The proton dissociation rate constant, k_{PT}, is determined from the exponential decay at early times of the fluorescence decay. At later times, the fluorescence decay is nonexponential due to the reversible geminate recombination.

An important parameter in our model that strongly influences the nonexponential decay is the mutual diffusion coefficient, $D = D_{H^+} + D_{RO^-}$. We are not aware of a pressure dependence study of the proton diffusion constant, D_{H^+} for propanol. The anion diffusion constant, D_{RO^-}, as a function of pressure, was estimated from the propanol viscosity dependence on pressure data.[46] The proton conductivity in neat propanol and water−propanol mixtures at atmospheric pressures was studied by Erdey-Gruz.[45] The prototropic conductance of propanol is small compared with water, methanol, and ethanol. We therefore assume that the proton diffusion constant decreases with pressure and the overall diffusion constant is an adjustable parameter in the fitting procedure. Figure 1 shows the viscosity dependence on pressure of propanol at 303 K taken from reference.[46] The empty symbols denote an extrapolation of the experimental data to higher pressures. For comparison we also display the viscosity dependence on pressure in water and ethanol.[46,47] In water, at 20 °C, the viscosity decreases slightly at low pressures. At high pressures (>2 kbar), the viscosity increases slightly. At higher temperatures, the minimum of the viscosity at low-pressure disappears and the viscosity increases with pressure. The viscosity of ethanol exhibits a larger pressure dependence than that of water. As seen in Figure 1, the pressure dependence viscosity of propanol is the largest of the three solvents. It increases by about 3 orders of magnitude at about 20 kbar. Another important parameter in the model is the Coulomb potential between the anion RO^-* and the geminate proton.

$$V(r) = -\frac{R_D}{r} \qquad R_D = \frac{|z_1 z_2| e^2}{\epsilon k_B T} \tag{2}$$

R_D is the Debye Radius, z_1 and z_2 are the charges of the proton and anion, ϵ is the static dielectric constant of the solvent, and T is the absolute temperature. e is the electronic charge, and k_B is Boltzmann's constant. The dielectric constant of ethanol and

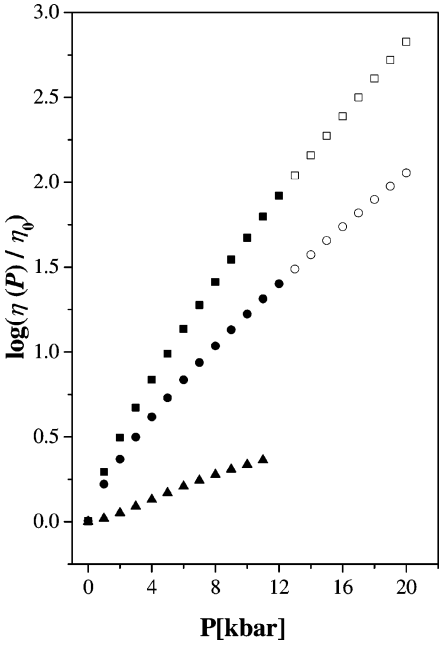

Figure 1. Viscosity dependence on pressure of propanol (■), ethanol (●), and water (▲) at 303 K taken from ref 46.

other polar liquids increases with pressure.[46] We are not aware of literature-published values for the dielectric constant as a function of pressure for propanol at higher pressures. We assume that the pressure dependence of the dielectric constant is similar to that of ethanol, which scales as the volume changes with pressure.

The asymptotic expression (the long time behavior) for the fluorescence of ROH*(t) is given by[48]

$$[\mathrm{ROH}^*] \cong \frac{\pi}{2} a^2 \exp(R_D/a) \frac{k_r}{k_{PT}(\pi D)^{3/2}} t^{-3/2} \qquad (3)$$

Equation 3 shows that uncertainty in the determination of $D(P)$ causes a larger uncertainty in k_r. Also, the fluorescence "background", due to a fluorescent impurity and the band overlap, prevents us from accurately determining the recombination rate constant. We estimate that the error in the determination of k_{PT} is 10%. This error is due to (1) the signal-to-noise ratio of the experimental signal, which affects the quality of the fluorescence signal over longer times and (2) the interplay between k_{PT} and k_r (see eq 2) over longer times. The uncertainty in the determination of k_r is estimated to be much larger, ∼50%. The relatively large uncertainty in the values of k_r arises from the relation between k_r, $D(P)$ and ϵ(P). In this paper, we focus our attention on the pressure dependence of the proton dissociation rate constant, $k_{PT}(P)$, which is measured quite accurately.

Figure 2 shows the steady-state emission of DCN2 in propanol at 0.77, 1.68, and 1.95 GPa. It is clearly seen that, as the pressure increases, the relative intensities of the ROH* emission band at 450 nm increases whereas the RO^-* band at 600 nm decreases with pressure increase. The changes in the emission spectra as a function of pressure are in qualitative agreement with the decrease of the proton-transfer rate constant, $k_{PT}(P)$, as a function of pressure.

Figure 3 shows, on a semilog scale, the experimental time-resolved emission intensity data of DCN2 in propanol, measured at 480 nm at various pressures in the range of 0.001−22 kbar. The experimental data are shown by symbols and the computer

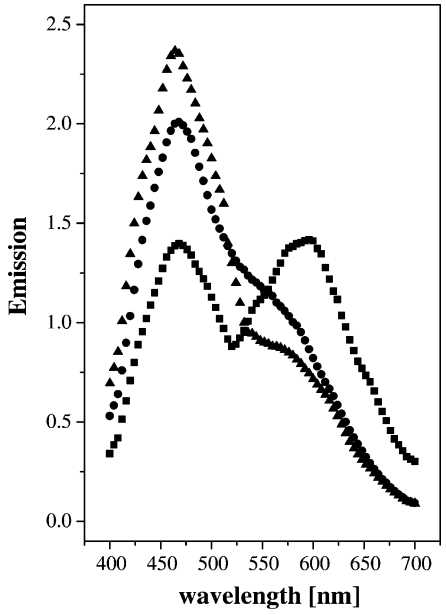

Figure 2. Steady-state emission of DCN2 in propanol at several pressures: (■) 0.77 GPa; (●) 1.68 GPa; (▲) 1.95 GPa.

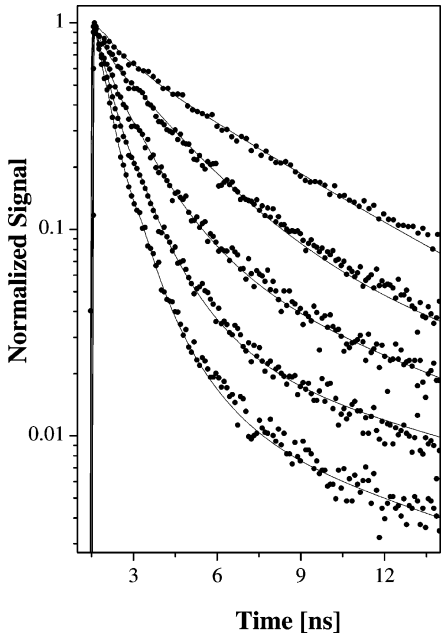

Figure 3. Experimental time-resolved emission intensity data (symbols) of DCN2 in a propanol solution measured at 480 nm at various pressures in the range 0.001−17 kbar along with the computer fit (solid lines). From top to bottom: 2.2, 1.7, 1.03, 0.75, and 0.0001 GPa.

fit by solid lines. We determined the proton-transfer rate constant, k_{PT}, from the fit to the initial decay of the ROH* fluorescence (∼500 ps for DCN2 in propanol at 1 atm, T = 298 K). The initial decay is mainly determined by the deprotonation process and is almost insensitive to the geminate recombination process. The long time behavior (the fluorescence tail) seen in the ROH* time-resolved emission is a consequence of the repopulation of the ROH* species by the reversible recombination of RO^-* with the geminate proton. As seen in the figure, over the high-pressure range 5−22 kbar, the emission decay rate of the fluorescence decreases as the pressure increases and, from the computer fit, we find that the proton-transfer rate constant, k_{PT}, decreases with pressure. The time-resolved emission also shows that above 10 kbar, the radiative lifetime increases with pressure.

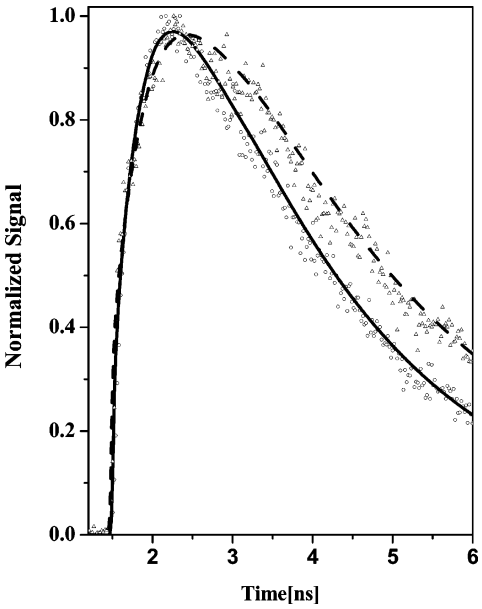

Figure 4. Time-resolved emission of a DCN2 RO^-* species in a propanol solution measured at 640 nm at atmospheric pressure (○) and at 1.36 GPa (△).

Figure 4 shows the time-resolved emission of the DCN2 RO^-* species in propanol measured at 640 nm at atmospheric pressure and at 1.3 GPa, along with the computer fit (solid line) using the reversible proton-transfer model. The parameters used in the fit of RO^-* luminescence are extracted from the fit of the fluorescence decay curves of the ROH* species, measured at 480 nm. The emission intensity at 640 nm has a growth time, which corresponds to the proton-transfer rate from the DCN2 ROH* species to water. The radiative decay time of the excited-state RO^-* depends only slightly on pressure (see Table 1).

Discussion

In the following section, we first present our stepwise two-coordinate proton-transfer model accounting for both the temperature and pressure dependence of the proton-transfer rate. We then correlate our model for proton transfer with the theory of nonadiabatic and adiabatic proton transfer.

A Qualitative Model for the Temperature and Pressure Dependencies of Excited-State Proton-Transfer Reactions. Previously, we used a qualitative model that accounts for both the temperature[8−11] and, recently,[34,35] pressure dependences of the excited-state intermolecular proton transfer to the solvent. We shall use the same model to explain the large pressure dependence of the proton-transfer rate from DCN2 to propanol (Table 1). The proton-transfer reaction depends on two coordinates, the first of which depends on a generalized solvent configuration. The solvent-coordinate characteristic time is within the range of the dielectric relaxation time, τ_D, and the longitudinal relaxation time, $\tau_L = (\epsilon_\infty/\epsilon_s)\tau_D$. The second coordinate is the actual proton translational motion (tunneling) along the reaction path. In our case the proton moves away from the oxygen, belonging to the hydroxyl group of DCN2, toward the oxygen of the propanol hydroxyl group.

The model restricts the proton-transfer process to a stepwise one. The proton moves to the adjacent hydrogen-bonded solvent molecule only when the solvent configuration brings the system to the crossing point (Scheme 1). In the stepwise model, the overall proton-transfer time is the sum of two times, $\tau = \tau_S + \tau_H$, where τ_S is the characteristic time for the solvent reorganization and τ_H is the time for the proton to pass to the acceptor. The overall temperature and pressure dependent rate constant, $k_{PT}(T,P)$, at a given T and P is

$$k_{PT}(T,P) = \frac{k_H(T,P)\, k_S(T,P)}{k_H(T,P) + k_S(T,P)} \tag{4}$$

where $k_S(T,P)$ is the solvent-coordinate rate constant and $k_H(T,P)$ is the proton-coordinate rate constant.

Equation 4 provides the overall excited-state proton-transfer rate constant along the lines of a stepwise process. As a solvent-coordinate rate constant, we use

$$k_S(T,P) = b\frac{1}{\tau_D(T,P)} \exp(-\beta\Delta G^{\ddagger}) \tag{5}$$

where $\beta = 1/k_BT$ and b is an adjustable empirical factor determined from the computer fit of the experimental data. We find that the empirical factor for monols lies between 2 and 4 whereas for water it is larger and lies between 4 and 8. For the monols, τ_L is usually smaller than τ_D by a factor of 2−6 and, for water, by about a factor of 10. Thus, the solvent characteristic time, $\tau_S = 1/k_S(T,P)$, for water and monols lies between the dielectric relaxation and longitudinal times, $\tau_L < \tau_S < \tau_D$. The activation energy, $\Delta G^{\ddagger}$, is usually determined by the Marcus relation using eq 16. Thus, one needs to know the excited-state acid equilibrium constant, K_a*, and the solvent reorganization energy. An alternative expression for $\Delta G^{\ddagger}$ can be evaluated from the structure reactivity relation of Agmon and Levine.[49] In our treatment, we assume that $\Delta G^{\ddagger}$ is independent of the hydrostatic pressure and hence the pressure solely affects the preexponential factor. In a previous study on the temperature dependence of the proton-transfer rate from DCN2 to alcohols,[34] we found that the activation energy for DCN2 to propanol is $\Delta G^{\ddagger} = 5$ kJ/mol. This value agrees qualitatively with the Marcus expression for the activation energy (see eq 16). The pK* value of DCN2 in water is estimated from the Forster cycle[2] to be ∼−4.

The reaction rate constant, k_H, along the proton coordinate, Q_H, is expressed by the usual activated chemical reaction description given by

$$k_H(P) = k_H^0(P) \exp(-\beta\Delta G^{\ddagger}) \tag{6}$$

where $k_H^0(P)$ is a pressure dependent preexponential factor and $\Delta G^{\ddagger}$ is the activation energy. The proton transfer occurs between

TABLE 1: Pressure Dependence of the Kinetic Parameters for the Proton-Transfer Reaction of DCN2 in Propanol

$P^{a,b}$ (GPa)	$10^{-9}k_{PT}{}^{c}$ (s^{-1})	$10^{-9}k_r{}^{c,d}$ (Å s^{-1})	$10^{-5}D^{e}$ ($cm^2\ s^{-1}$)	$\tau^{-1}_{RO^-*}$ (ns^{-1})	τ^{-1}_{ROH-*} (ns^{-1})
0.0001	1.90	2.4	14.0	0.47	0.33
0.18	2.00	2.4	9.0	0.50	0.34
0.28	2.30	2.5	8.0	0.50	0.34
0.36	2.20	2.5	7.5	0.50	0.34
0.57	1.90	2.5	5.0	0.50	0.34
0.75	1.50	2.6	4.5	0.50	0.34
1.03	0.95	2.4	3.0	0.47	0.34
1.30	0.80	2.3	2.0	0.43	0.32
1.68	0.43	2.3	0.9	0.40	0.30
2.20	0.08	2.3	0.7	0.40	0.25

[a] 1Gpa ∼ 10 kbar. [b] The error in determination of the pressure is ±0.075 Gpa. [c] k_{PT} and k_r are obtained from the fit of the experimental data by the reversible proton-transfer model (see text). [d] The error in the determination of k_r is 50%; see text. [e] Values at high pressure obtained by best fit to the fluorescence decay.

the hydroxyl group of DCN2 and the adjacent oxygen of a hydrogen-bonded propanol molecule. In alcohols, at high temperatures, or water with relatively large relaxation rates (τ_D = 8 ps, at 293 K), the actual proton transfer along the proton tunneling coordinate, Q_H, is the slower process, and hence the rate determining step. $k_H^0(p)$ depends strongly on pressure because tunneling in the intermediate coupling case depends exponentially on the intermolecular distance between the two heavy atoms. In propanol, the solvent relaxation is slow and also depends strongly on the pressure. The overall proton-transfer rate at high pressures is determined by k_S, which decreases with pressure.

As we shall show in the next section, $k_H(P)$ is related to the nonadiabatic limit rate expression. In the nonadiabatic limit, the preexponential factor, is related to the tunneling coupling matrix element (see eq 14). The coupling matrix element depends strongly on and increases with, pressure.

The effect of pressure and temperature on the photoinduced hydrogen-transfer reaction in a mixed crystal of acridine in fluorene was studied by Bromberg et al.[50] The room temperature hydrogen-transfer rate increases exponentially with pressure. On the basis of proton tunneling concepts, Trakhtenberg and Klochikhin[31] derived an expression for the pressure and temperature dependence of the tunneling rate of proton transfer in the solid state:

$$k(P,T) = \nu \exp[-J(R_0) + J'R_0(1 - \alpha_P^{-1/3}) + J'^2\delta_{CN}{}^2/8\alpha_P{}^{\gamma} \coth(\hbar\Omega_0\alpha_P{}^{\gamma}/4k_BT)] \quad (7)$$

where υ is the preexponential factor, $\alpha_P(P) = V_0/V(P)$, Ω_0 is the effective frequency of the intermolecular vibration, $\delta_{CN}{}^2$ is the square of the amplitude of the intercenter C···N distance, and $\gamma = -\partial \ln \Omega_0/\partial \ln V$.

$$J(R) = (2/\hbar)\int\{2m[U(x,R) - E_H(R)]\}^{1/2}dx \quad (8)$$

$E_H(R)$ and $U(x,R)$ are the total and potential energies of the tunneling atom, respectively, depending on the distance, R, between the two heavy atoms (in our case two oxygen atoms). R_0 is the equilibrium distance between the heavy atoms, and J' is the derivative, $\partial J/\partial R$. The first term on the right-hand side of eq 7 is the tunneling expression at atmospheric pressure and does not account for the pressure effect. The second term accounts for the change in the rate with pressure because of the change in the equilibrium position between the two heavy atoms. The third term takes into account the pressure effect on the intermolecular low frequency.

For the first approximation, the change in distance between the oxygen atoms is $\delta Q_H = \sqrt[3]{\Delta V}$, where ΔV is the change in volume at a particular pressure. Trakhtenberg et al.[31] found good correspondence with the experimental results of Bromberg et al.[50] when they used a smaller power dependence of the compressibility, $\alpha_P = 0.22$, instead of $^1/_3$, as expected from the relation of distance and volume. In our previous pressure study of DCN2 in ethanol, we estimated the pressure dependence of the proton-coordinate rate constant, $k_H(P)$, from the second term of eq 6 with a compressibility dependence on a power of 0.22. In our previous work[35] on the pressure effect in 2N6S−water, we used the value of 0.33. In the current work, we used a value of 0.27.

$$\frac{k_H(P)}{k_H(1\text{ atm})} \cong \exp[J'R_0(1 - \alpha_P^{-0.27})] \quad (9)$$

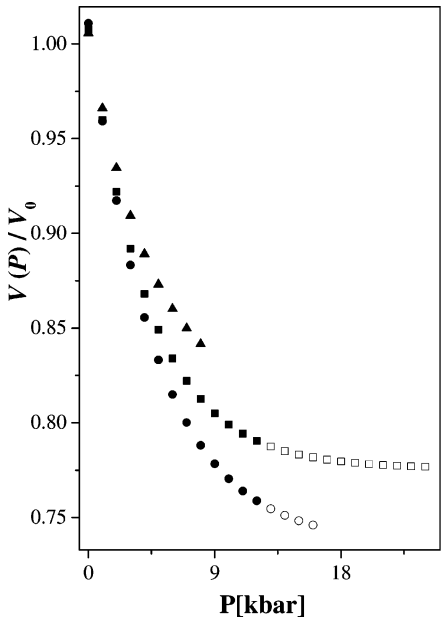

Figure 5. Pressure dependence of $1/\alpha_P = V_P/V_0$ of propanol (■), ethanol (●), and water (▲).

In our treatment, we neglected the contribution to the pressure dependence of the third term rate constant in eq 7, which we estimate to be significantly smaller.[31]

Figure 5 shows the dependence of $1/\alpha_P = V_P/V_0$ on pressure, for propanol and, for comparison, we also added the pressure dependence of $1/\alpha_P$ for ethanol and water, where the V_P's of both liquids are taken from ref 46. The empty symbols denote an extrapolation of the experimental data to higher pressures. In water, alcohols and many other liquids, the change in volume with pressure over a pressure range up to 10 kbar is very similar. The compressibility

$$\frac{1}{V}\left(\frac{\partial V}{\partial P}\right)_T$$

decreases with pressure. In general, it is smaller for water than for methanol and ethanol. For water and ethanol it changes by a factor of about 3 and 5 between atmospheric pressure and 10 kbar, respectively. Figure 6 shows the pressure dependence of the proton tunneling rate constant, using eq 9, and the following parameters, $J' = 10.4$ Å^{-1}, $R_0 = 2.4$ Å, $J'R_0 = 25$. α_P was taken from ref 46. As seen, the rate increases as a function of pressure. Because $1/\alpha_P$ is not constant with pressure, but rather decreases as the pressure increases, $k_H(P)/k_H(1\text{ atm})$ does not increase with the same initial slope.

In previous studies,[8−13] we used the longest component of the dielectric relaxation time, τ_D, for the solvent-coordinate preexponential factor of the rate constant, $k_S = b/\tau_D \exp(-\Delta G^{\ddagger}/RT)$, where b is an empirical factor. For water, we found $b \approx 6$ and, for all monols studied, the value is less, $2 < b < 4$. We are not aware of literature-published values for the dielectric relaxation times as a function of pressure for propanol at higher pressures up to the freezing pressure of ~10 kbar. In many cases the viscosity and τ_D have similar dependencies on both pressure and temperature. As seen in Figure 1, the viscosity dependence on the pressure of propanol at 30 °C is very large, whereas in ethanol the dependence is smaller and for water it is very small.

The dielectric relaxation time is often directly proportional to the shear viscosity. This is a direct consequence of the assumed viscous-damped rotating sphere model of dielectric

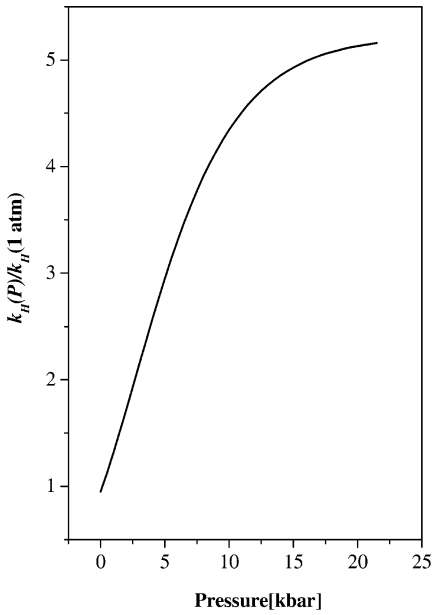

Figure 6. Pressure dependence of the proton tunneling rate constant, using eq 9. Parameters: $J' = 10.4$ Å^{-1}, $R_0 = 2.4$ Å.

relaxation originally introduced by Debye.[43] In general, the viscosity dependence on pressure is larger than that of the dielectric relaxation. Johari and Danhauser studied the pressure dependence of the viscosity and the dielectric relaxation of isomeric octanols.[51,52] They found good correspondence between the pressure dependence of the viscosity and dielectric relaxation times.

We used an approximate relation between $\tau_D(P)$ and $\eta(P)$ based on the correspondence between dielectric relaxation and $\eta(P)$ to estimate the pressure dependence of the $\tau_D(P)$ of propanol.

$$\tau_D(P) \sim \tau_D^{1atm}\left(\frac{\eta(P)}{\eta^{1atm}}\right)\exp(-P/P^*) \qquad (10)$$

For the best fit to the pressure dependence of k_{PT} using our stepwise model, we used $P^* = 6000$ bar.

Figure 7a shows a fit to the stepwise two-coordinate model of

$$k_{PT}(P) = \frac{k_H(P)\,k_S(P)}{k_H(P) + k_S(P)}$$

as a function of pressure (solid line) along with the experimental data (dots). The results of DCN2 in propanol show a slight increase of the proton-transfer rate with pressure changes up to about 5 kbar. At pressures above 5 kbar (0.5 GPa), the rate decreases as a function of pressure. In Figure 7b we also show, for comparison, the pressure dependence of DCN2 in ethanol taken from our previous study[34] and the pressure dependence of 2NP6S in water.[35] The results of DCN2 in ethanol show an initial significant increase of the rate with the pressure. At about 8 kbar the rate reaches a maximum value, $k_{PT}(8\text{ kbar}) = 2k_{PT}(1\text{ atm})$. Further increase of the pressure decreases the rate constant of the proton transfer to the solvent. This interesting observation of the pressure dependence of the proton-transfer rate from DCN2 to ethanol is explained by the opposite pressure dependencies of k_H and k_S and the saturation of k_H at medium-pressure values. The pressure dependence of k_{PT}, k_H, and k_S for DCN2 in propanol, 2-naphthol-6-sulfonate in water, and DCN2 in ethanol are also plotted (dotted lines) in Figure 7a−c, respectively. The explanation for the large difference in the pressure dependence of the proton-transfer rate from DCN2 to propanol, 2-naphthol-6-sulfonate to water, and DCN2 to ethanol is given along the lines of the two-coordinate model in the next section.

Qualitative Comparison of the Pressure Dependence of Proton Transfer with the Landau−Zener Curve Crossing Formulation. In this section, we compare our qualitative model, based on the pressure and temperature dependences of the proton-transfer rate, with the Landau−Zener curve crossing formulation.

The reactant is an intermolecular hydrogen-bonded complex between the excited photoacid, AH*, and a solvent molecule, S_B, that serves as a base, characterized by a hydrogen bond to the photoacid and also other solvent molecules. In water, this specific solvent molecule, S_B, has three hydrogen bonds to three water molecules. To form the product, $A^-{}^*\cdots HS_B^+$, in water, one hydrogen bond, of S_B to a water molecule, must break. Thus, relatively long-range reorganization of the hydrogen bond network takes place upon proton transfer to the solvent. This complex rearrangement, to accommodate the product in water and alcohols, is probably the reason for a slow solvent-generalized configuration motion, which corresponds to a low-frequency component in the solvent dielectric spectrum. Its time constant is close to the slowest component of the dielectric relaxation time. According to Kuznetsov,[17] Borgis and Hynes,[19] Bernstein and co-workers,[53] Syage,[54] and Trakhtenberg,[31] a second important coordinate should be taken into account. This second coordinate is the distance between the two heavy atoms, in our case O−H···O, and Q_H is the relevant proton coordinate. This distance is modulated by a low-frequency vibrational mode, Ω_0[19,31,53] (about 200 cm^{-1}). The proton tunnels through the barrier from the reactant well to the product well via the assistance of the low frequency, Ω_0, mode whenever the solvent configuration equalizes the energies of the reactant and the product. Free energy relation[55,56] and temperature and pressure dependence experiments[10] indicate that the solvent fluctuation rate to equalize the energies is not in the high-frequency range of the order of 10^{13} s^{-1}, (∼100−200 cm^{-1}), but slower than 10^{12} s^{-1} (<10 cm^{-1}). For monols, diols, and glycerol, it is very close to $1/\tau_D$, where τ_D is the slow component of the dielectric relaxation time. For alcohols, the solvent fluctuation rate is about 2−4 times larger than $1/\tau_D$.

The proton-transfer rate constant, k_{PT}, between the reactant and product can be expressed as the average one-way flux in the solvent coordinate, through the crossing point S* of the two free energy curves[19] with the inclusion of the Landau−Zener transmission coefficient, κ_{LZ}, giving the probability of a successful curve crossing:

$$k_{PT} = \langle \dot{S}\Theta(\dot{S})\,\delta(S-S^*)\,\kappa_{LZ}(\dot{S},S^*)\rangle_R \qquad (11)$$

where S is the solvent coordinate, $\dot{S}$ is the solvent velocity, and $\Theta(\dot{S})$ the positive velocity step function. Here the average is over the classical solvent distribution, normalized by the partition function of the solvent in the reactant region.

The LZ transmission factor, appropriate for a positive velocity approach to the crossing point, is

$$\kappa_{LZ} = [1-1/2\,\exp(-\gamma)]^{-1}[1-\exp(-\gamma)] \qquad (12)$$

$$\gamma = \frac{2\pi C^2}{\hbar(\partial\Delta V/\partial S)_{S^*}\dot{S}} = \frac{2\pi C^2}{\hbar k_{S^*}\dot{S}} \qquad (13)$$

κ_{LZ} includes multiple pass effects on the transition probability.

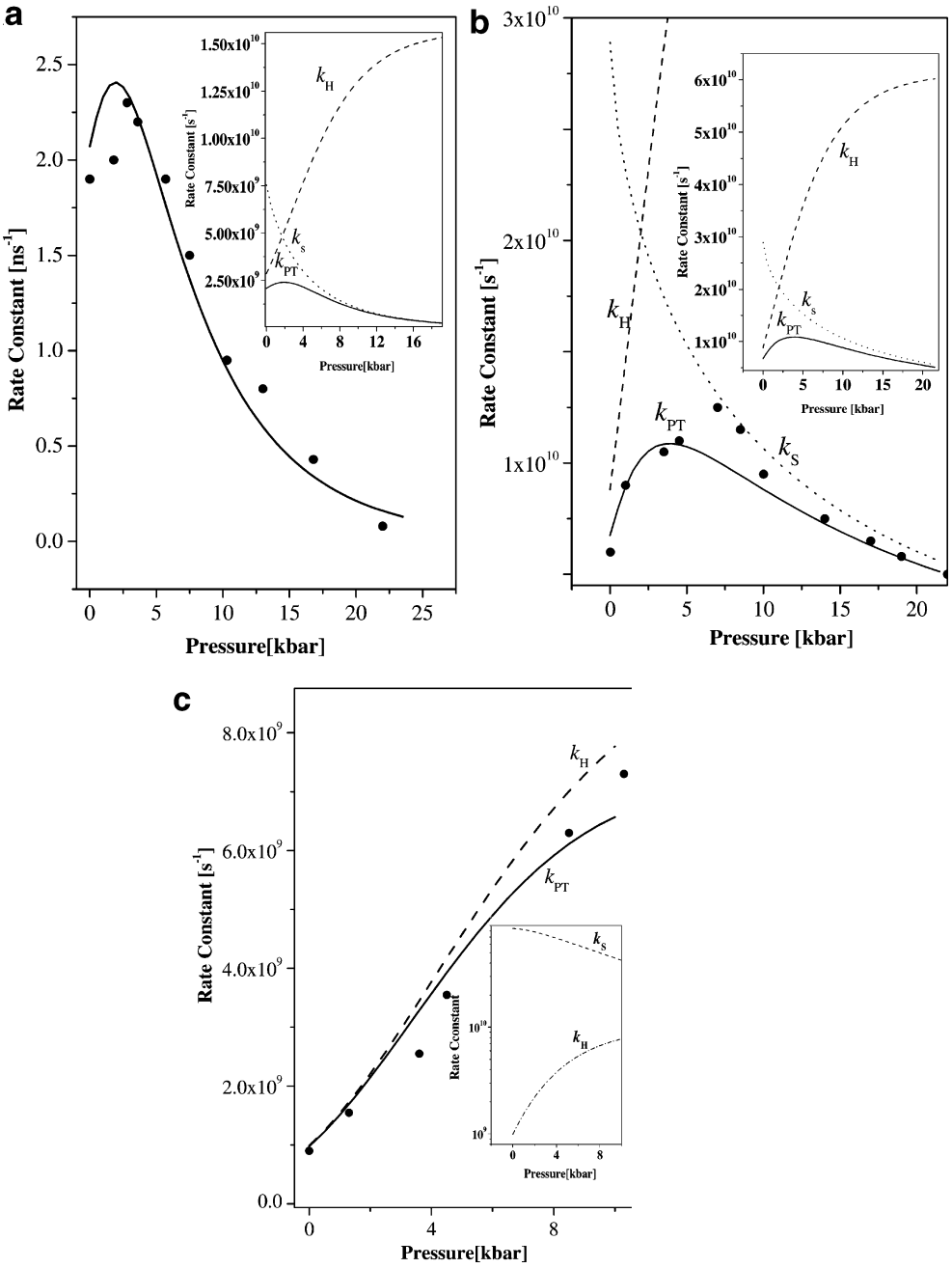

Figure 7. Fit to the stepwise two-coordinate model of $k_{PT}(P) = [k_H(P)\, k_S(P)]/[k_H(P) + k_S(P)]$ as a function of pressure (solid line) along with the experimental data (●): (a) DCN2 in propanol; (b) DCN2 in ethanol; (c) 2-nphthol-6-sulfonate in water (semilog scale). $k_H(P)$ and $k_S(P)$ are shown as dashed and dotted lines, respectively. Inset: calculated rate constants.

(Note that $\kappa_{LZ} \rightarrow 1$ is the adiabatic limit). When $\gamma \ll 1$, one obtains the nonadiabatic limit result

$$\kappa_{LZ} = 2\gamma \tag{14}$$

This leads to

$$k_{PT}^{NA} = \frac{2\pi}{\hbar} C^2 \left(\frac{\beta}{4E_S\pi}\right)^{1/2} e^{-\beta\Delta G^{\ddagger}} \tag{15}$$

in which $\Delta G^{\ddagger}$ is the activation free energy

$$\Delta G^{\ddagger} = \frac{1}{4E_S}(E_S + \Delta G)^2 \tag{16}$$

In the nonadiabatic limit, the preexponential term depends on C^2. C depends exponentially (eq 1) on the distance between the two oxygens (the hydroxyl group and that of the hydrogen bonded solvent molecule). γ (eq 13) depends on three parameters: the potential surfaces curvature, $(\partial\Delta V/\partial S)_{S^*}$, C^2, and $\dot{S}$. C^2 depends strongly on pressure (see eq 7) via the internuclear distance, Q_H, and the intermolecular vibrational mode, Ω_0, depends, to a lesser extent, on pressure. The solvent velocity, $\dot{S}$, depends strongly on both the temperature and pressure. On the basis of the experimental data and the qualitative stepwise model of the pressure and temperature dependence of the proton-transfer rate constant, we infer that $\dot{S} = b/\tau_D$, where τ_D is the solvent dielectric relaxation time and b is a factor of about 6 in water and between 2 and 4 in monols.

For the alcohols used in the experiments of Ref. 9, the value of γ as a function of the temperature smoothly increases from a value close to 0, i.e., $\gamma < < 1$ (the nonadiabatic limit) to a value $\gamma \gg 1$ (the adiabatic limit). An illustration of the pressure

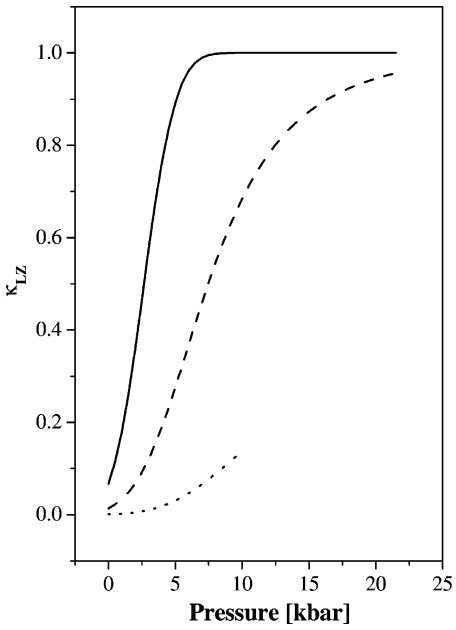

Figure 8. Pressure dependence of the transmission coefficient, κ_{LZ}, for DCN2 in propanol (solid line), for 2-naphthol-6-sulfonate in a water[35] (dotted line) solution, and for DCN2 in ethanol[34] (dashed line) as a function of pressure.

dependence of the transmission coefficient, κ_{LZ}, for proton transfer from DCN2 to propanol, DCN2 to ethanol,[34] and also 2-naphthol-6-sulfonate to a water solution is shown in Figure 8. We used eqs 12 and 13 and assumed that the pressure dependence of the coupling matrix element can be given for DCN2 to ethanol and propanol by

$$C = C_0 \exp\{0.5[J'R_0(1 - \alpha_P^{-0.27})]\} \qquad (17)$$

Eq 17 is similar to eq 1 and uses the second term of Trakhtenberg's pressure dependence of the proton-tunneling rate. In Figure 8, we used $2\pi C_0^2/\hbar k_{S*} = 3 \times 10^8$ for three proton-transfer reactions. For DCN2 in propanol, κ_{LZ} changes rapidly with pressure from close to zero at atmospheric pressure to close to 1 at 5 kbar. For 2-naphthol-6-sulfonate to water, κ_{LZ} changes from close to zero at low pressures to only about 0.15 at 10 kbar, the water−ice VI phase transition. κ_{LZ}, as a function of pressure, for DCN2 to ethanol, changes from close to zero at low pressure to a value close to 1 at about 19 kbar the liquid−solid-phase transition of ethanol. For DCN2 in both propanol and ethanol, the proton-transfer rate changes as a function of pressure from the nonadiabatic regime, $\kappa_{LZ} \ll 1$, at low pressures to the solvent control regime at the high-pressure limit. For the three cases discussed, the coupling matrix element C increases with pressure. For 2N6S in water, C^2 increases by about a factor of 10 at 10 kbar. For DCN2 in propanol and ethanol, C^2 increases by about a factor of 6. This effect tends to increase γ with pressure. The pressure dependence of τ_D affects γ in the same direction. The overall effect of pressure on γ is a rapid increase with pressure. In propanol and ethanol, the solvent dielectric relaxation time is relatively slow, $\tau_D = 340$ and 120 ps at atmospheric pressure, respectively. It decreases strongly with pressure and γ (see eq 13) increases with pressure. At high pressures, $\kappa_{LZ} \approx 1$, the proton-transfer rate follows the solvent relaxation rate and also decreases at the high-pressure limit. In contrast to alcohols, the proton transfer from 2-naphthol-6-sulfonate to water is almost a nonadiabatic reaction over the entire pressure range. τ_D in water is relatively fast, $\tau_D = 8$ ps, and exhibits a relatively small pressure dependence. γ increases with pressure, but its absolute value is small at all pressures. The solvent-controlled limit is not reached even at the highest pressure, 10 kbar. Therefore tunneling prevails and the rate increases with pressure.

Our stepwise model[9−13] is similar to the expression of Rips and Jortner[57] for the overall ET rate constant that bridges between the two extreme cases: the nonadiabatic and adiabatic ET. The expression that bridges between the nonadiabatic and solvent-controlled adiabatic limit for the proton transfer to the solvent is

$$k_{PT}(T,P) = \frac{k_{PT}^{NA}(T,P)\, k_{PT}^{AD}(T,P)}{k_{PT}^{NA}(T,P) + k_{PT}^{AD}(T,P)} \qquad (18)$$

This equation has a form similar to that of eq 4, which we used to fit the experimental data. To use the rate constants quantitatively, we face some unknown parameters. The rate constant for the nonadiabatic proton-transfer includes the unknown coupling matrix, C. We do not know the absolute value of the coupling matrix element but we can express its pressure dependence and reformulate (eq 15).

$$k_{PT}^{NA}(P) = k_{PT}^{NA}(1 \text{ atm}) \exp[-J'R_0(1 - \alpha^{-\delta})] \qquad (19)$$

where $k_{PT}^{NA}(1 \text{ atm})$ is given by eq 15 and δ is an adjustable parameter. For the adiabatic limit, Borgis and Hynes found[19] that

$$k_{PT}^{AD} = \left(\frac{\omega_S}{2\pi}\right) \exp(-\beta \Delta G_{AD}^{\ddagger}) \qquad (20)$$

The formal expressions for the pressure dependence of k_{PT}^{NA} and k_{PT}^{AD} are given by eqs 19 and 20. k_{PT}^{NA} is qualitatively parallel to k_H in eq 4. Accordingly, the preexponential factor depends on the pressure. k_{PT}^{AD} has a similar form to k_S in eq 5, but we replace the high frequency, $\omega_S/2\pi$, in eq 5 with the slow dielectric relaxation time, τ_D. The time scale of the solvent control is slow and close to τ_D. Using eq 18 to calculate $k_{PT}(T,P)$ as a function of the pressure results in similar behavior to eq 4. Figure 7a shows the fit to the experimental proton-transfer rate from DCN2 to propanol using eq 4. As seen, the fit is good. For DCN2 in propanol at atmospheric pressure, k_S is comparable with k_H. When $k_H = k_S$, $k_{PT} = {}^1/_2 k_H$. As the pressure increases, k_S decreases and k_H increases at about the same rate. Thus, according to eq 4, the overall rate will be almost independent of pressure. As the pressure increases further, the solvent coordinate rate further decreases and the rate-limiting step is the solvent rate and k_{PT} will follow k_S. For 2N6S in water, the tunneling rate constant, in our model k_H, increases with pressure, from atmospheric pressure to 10 kbar, by a factor of 10. The value of the solvent-coordinate rate constant of water, k_S, at atmospheric pressure, $k_S \sim 10^{12}$ s^{-1} is larger by about 2 orders of magnitude than $k_H = 10^{10}$ s^{-1}. Although k_H increases 10-fold with pressure, k_S decreases with pressure by only a factor of 2. Because $k_S \gg k_H$ at all pressures, the value of the overall rate constant (eq 4), k_{PT}, is mainly determined by the slowest rate constant, i.e., k_H. Therefore, the total rate, $k_{PT}(T,P)$, increases with pressure by a factor of 8 at about 1 GPa, the water−ice VI transition point.

Summary

DCN2 is a strong photoacid capable of transferring a proton not only to water, but also to other protic solvents. We studied, using time-resolved emission techniques, the proton dissociation

and reversible proton geminate recombination processes as a function of pressure of DCN2 in propanol. The experimental time-resolved fluorescence data are analyzed by the exact numerical solution of the transient Debye−Smoluchowski equation (DSE). We found that the proton dissociation rate constant, k_{PT}, of excited DCN2 in neat propanol at relatively low pressures (up to 5 kbar) increases slightly with pressure. At 5 kbar the rate is 20% larger than the value at atmospheric pressure. At higher pressures, up to ∼2.5 GPa (25 kbar), the proton-transfer rate decreases with pressure and its value is related to the inverse of the dielectric relaxation time. At about 2.2 GPa, the rate is smaller by a factor of about 20 than at atmospheric pressure.

We compared these results with our previous pressure work on DCN2 in ethanol, for which the proton-transfer rate first increased as a function of pressure and subsequently decreased as the pressure further increases. We also compared these results with our recent studies of proton transfer from the photoacid 2-naphthol-6-sulfonate (2N6S) to water as a function of pressure. For 2N6S we found that the proton dissociation rate constant, k_{PT}, up to the pressure of the freezing point (∼10 kbar), increases by about a factor of 8 with pressure.

We used a stepwise two-coordinate model to qualitatively fit the pressure dependence of the proton-transfer rate in all three cases. The model predicts that the overall proton-transfer rate will be determined by both the proton tunneling rate, k_H, and the solvent relaxation rate, k_S. In the case of DCN2 in propanol, the increase in the proton tunneling rate, k_H, at low pressure, slightly increases the overall rate, k_{PT}. The solvent-coordinate rate, k_S, strongly affects k_{PT} at high pressures. At pressures above 5 kbar, k_{PT} is mainly determined by k_S, i.e., the solvent-controlled limit. In contrast to DCN2−propanol, in the case of proton transfer from 2-naphthol-6-sulfonate to water, pressure only mildly affects the solvent-coordinate rate of water, k_S, whereas the tunneling rate, k_H, increases almost 10-fold with pressure. The overall effect is a strong increase of the proton-transfer rate, k_{PT}, with pressure. The pressure dependence of DCN2 in ethanol is an intermediate case where both coordinates, the generalized solvent and the proton tunneling, strongly affect the overall proton-transfer rate constant, k_{PT}. At low pressures, up to about 8 kbar, k_{PT} increases with pressure. At higher pressures, $P > 8$ kbar, k_{PT} decreases with pressure. Thus, at low pressures, k_H is the rate-limiting step whereas, at high pressures, the solvent fluctuation rate, k_S, is the rate determining step.

Acknowledgment. We thank Prof. L. Tolbert for providing the 5,8-dicyano-2-naphthol. We thank Prof. M. Pasternak and Dr. G. Rozenberg for providing the diamond anvil cell high-pressure technology. This work was supported by grants from the US-Israel Binational Science Foundation and the James-Franck German-Israel Program in Laser-Matter Interaction.

References and Notes

(1) Ireland, J. F.; Wyatt, P. A. H. *Adv. Phys. Org. Chem.* **1976**, *12*, 131.

(2) Weller, A. *Prog. React. Kinet.* **1961**, *1*, 187.

(3) Huppert, D.; Gutman, M.; Kaufmann, K. J. In *Advances in Chemical Physics*; Jortner, J., Levine, R. D., Rice, S. A., Eds.; Wiley: New York, 1981; Vol. 47, p 681. Kosower, E. M.; Huppert, D. In *Annual Reviews of Physical Chemistry*; Strauss, H. L., Babcock, G. T., Moore, C. B. Eds.; Annual Reviews Inc.: California, 1986; Vol. 37, p 122.

(4) Lee, J.; Robinson, G. W.; Webb, S. P.; Philips, L. A.; Clark, J. H. *J. Am. Chem. Soc.* **1986**, *108*, 6538.

(5) Gutman, M.; Nachliel, E. *Biochim. Biophys. Acta* **1990**, *391*, 1015.

(6) Knochenmuss, R. *Chem. Phys. Lett.* **1998**, *293*, 191.

(7) Peters, S.; Cashin, A.; Timbers, P. *J. Am. Chem. Soc.* **2000**, *122*, 107.

(8) Poles, E.; Cohen, B.; Huppert, D. *Isr. J. Chem.* **1999**, *39*, 347.

(9) Cohen, B.; Huppert, D. *J. Phys. Chem. A* **2001**, *105*, 2980.

(10) Cohen, B.; Huppert, D. *J. Phys. Chem. A* **2002**, *106*, 1946−1955.

(11) Cohen, B.; Segal, J.; Huppert, D. J. *Phys. Chem. A* **2002**, *106*, 7462.

(12) Cohen, B.; Leiderman, P.; Huppert D. *J. Phys. Chem. A* **2002**, *106*, 11115.

(13) Cohen, B.; Leiderman, P.; Huppert, D. *J. Phys. Chem. A* **2003**, *107*, 1433.

(14) Kolodney, E.; Huppert, D. *J. Chem. Phys.* **1981**, *63*, 401

(15) Ando, K.; Hynes, J. T. In *Structure, energetics and reactivity in aqueous solution*; Cramer, C. J., Truhlar, D. G., Eds.; American Chemical Society: Washington, DC, 1994. Ando, K.; Hynes, J. T. *J. Phys. Chem. B* **1997**, 101, 10464.

(16) Agmon, N.; Huppert, D.; Masad, A.; Pines, E. *J. Phys. Chem.* **1991**, *96*, 952.

(17) German, E. D.; Kuznetsov, A. M.; Dogonadze, R. R. J. *Chem. Soc., Faraday Trans. 2* **1980**, *76*, 1128.

(18) Kuznetsov, A. M. *Charge Transfer in Physics, Chemistry and Biology*; Gordon and Breach, SA: Luxembourg, 1995.

(19) Borgis, D.; Hynes, J. T. *J. Phys. Chem.* **1996**, *100*, 1118. Borgis, D. C.; Lee, S.; Hynes, J. T. *Chem. Phys. Lett.* **1989**, *162*, 19. Borgis, D.; Hynes, J. T. *J. Chem. Phys.* **1991**, *94*, 3619.

(20) Cukier, R. I.; Morillo, M. *J. Chem. Phys.* **1989**, *91*, 857. Morillo, M.; Cukier, R. I. *J. Chem. Phys.* **1990**, *92*, 4833.

(21) Li, D.; Voth, G. A. *J. Phys. Chem.* **1991**, *95*, 10425. Lobaugh, J.; Voth, G. A. *J. Chem. Phys.* **1994**, *100*, 3039.

(22) Hammes-Schiffer, S. *Acc. Chem. Res.* **2001**, *34*, 273.

(23) Hammes-Schiffer *J. Phys. Chem. A* **1998**, *102*, 10443.

(24) Kreevoy, M. M.; Kotchevar, A. T. *J. Am. Chem. Soc.* **1990**, *112*, 3579. Kotchevar, A. T.; Kreevoy, M. M. *J. Phys. Chem.* **1991**, *95*, 10345.

(25) Asano, T.; le Noble, W. J. *Chem. Rev.* **1978**, *78*, 407.

(26) Kelm, H., Ed. *High-Pressure Chemistry*; Reidel: Dordrecht, The Netherlands, 1978.

(27) le Noble, W. J.; Kelm, H. *Angew. Chem., Int. Ed. Engl.* **1980**.

(28) Van Eldik, R.; Asano, T.; le Noble, W. *J. Chem. Rev.* **1989**, *89*, 549.

(29) Rollinson, A. M.; Drickamer, H. G. *J. Chem. Phys.* **1980**, *73*, 5981.

(30) Schroeder, J. *J. Phys. Condens. Matter* **1996**, *8*, 9379.

(31) Trakhtenberg, L. I.; Klochikhin, V. L. *Chem. Phys.* **1998**, *232*, 175.

(32) Goldanskii, V. I.; Trakhtenberg, L. I.; Fleuorov, V. N. *Tunneling Phenomena in Chemical Physics*; Gordon and Breach, New York, 1989; Chapter IV.

(33) Huppert, D.; Jayaraman, A.; Maines Sr., R. G.; Steyert, D. W.; Rentzepis, P. M. *J. Chem. Phys.* **1984**, *81*, 5596.

(34) Koifman, N.; Cohen, B.; Huppert, D. *J. Phys. Chem. A* **2002**, *106*, 4336.

(35) Leiderman, P.; Genosar, L.; Koifman, N.; Huppert, D. Submitted to *J. Phys. Chem A.*

(36) Jayaraman, A. *Rev. Mod. Phys.* **1983**, *55*, 65.

(37) Machavariani, G. Yu.; Pasternak, M. P.; Hearne, G. R.; Rozenberg, G. Kh. *Rev. Sci. Instrum.* **1998**, *69*, 1423.

(38) D'ANVILS is administered by Ramot Ltd., 32 H. Levanon Str., Tel Aviv 61392, Israel. http://www.tau.ac.il/ramot/danvils.

(39) Barnett, J. D.; Block, S.; Piermarini, G. J. *Rev. Sci. Instum.* **1973**, *44*, 1.

(40) Tolbert, L. M.; Haubrich, J. E. *J. Am. Chem. Soc.* **1990**, *112*, 8163. Tolbert, L. M.; Haubrich, J. E. *J. Am. Chem. Soc.* **1994**, *116*, 10593.

(41) Pines, E.; Huppert, D.; Agmon, N. *J. Chem. Phys.* **1988**, *88*, 5620.

(42) Agmon, N.; Pines, E.; Huppert, D. *J. Chem. Phys.* **1988**, *88*, 5631.

(43) Debye, P. *Trans. Electrochem. Soc.* **1942**, *82*, 265.

(44) Krissinel, E. B.; Agmon, N. *J. Comput. Chem.* **1996**, *17*, 1085.

(45) Erdey-Gruz, T.; Lengyel, S. In *Modern Aspects of Electrochemistry*; Bockris, J. O'M., Conway, B. E., Eds.; Plenum: New York, 1964; Vol. 12, pp 1−40.

(46) Bridgman, P. E. *The Physics of High Pressure*; G. Bell and Sons Ltd.: London, 1958.

(47) Andrussow, L.; Schramm, B. *Landolt-Bornstein*; Schaffer, K., Ed.; Springer: Berlin, 1969; Vol. 2, Part 5a.

(48) Agmon, N.; Goldberg, S. Y.; Huppert, D. *J. Mol. Liq.* **1995**, *64*, 161.

(49) Agmon, N.; Levine, R. D. *Chem. Phys. Lett.* **1977**, *52*, 197. Agmon, N.; Levine, R. D. *Isr. J. Chem.* **1980**, *19*, 330.

(50) Bromberg, S.; Chan, I.; Schilke, D.; Stehlik, D. *J. Chem. Phys.* **1993**, *98*, 6284.

(51) Johari, G.; Dannhauser, W. *J. Chem. Phys.* **1969**, *50*, 1862.

(52) Johari, G.; Dannhauser, W. *J. Chem. Phys.* **1969**, *51*, 1626.

(53) Hineman, M. F.; Brucker G. A.; Kelley D. F.; Bernstein E. R. *J. Chem. Phys.* **1992**, *97*, 3341.

(54) Syage, J. A. *J. Phys. Chem.* **1995**, *99*, 5772.

(55) Pines, E.; Fleming, G. R. *Chem. Phys. Lett.* **1994**, *183*, 393. Pines, E.; Magnes, B.; Lang, M. J.; Fleming, G. R. *Chem. Phys. Lett.* **1997**, *281*, 413.

(56) Solntsev, K.; Huppert, D.; Agmon, N. *J. Phys. Chem. A* **2000**, *104*, 4658.

(57) Rips, I.; Jortner, J. *J. Chem. Phys.* **1987**, *87*, 2090.